frontiers | Frontiers in Amphibian and Reptile Science

TYPE Original Research
PUBLISHED 28 January 2025
DOI 10.3389/famrs.2024.1503056

OPEN ACCESS

EDITED BY
Robert Puschendorf,
University of Plymouth, United Kingdom

REVIEWED BY
Brent Newman,
Centers for Disease Control and Prevention (CDC), United States
Santosh Mogali,
Karnatak University, India

*CORRESPONDENCE
Talon Jost
talonjost@gmail.com

RECEIVED 28 September 2024
ACCEPTED 16 December 2024
PUBLISHED 28 January 2025

CITATION
Jost T, Henderson A, LaBumbard B, Magori K, Stokes A, Bergin D, Holley A, Bletz M, Hernández-Gómez O, Bucciarelli G, Woodhams DC, Piovia-Scott J and Walke JB (2025) Tetrodotoxin, fungal pathogen infection, and bacterial microbiome associations are variable in the skin microecosystems of two *Taricha* newt species.
Front. Amphib. Reptile Sci. 2:1503056.
doi: 10.3389/famrs.2024.1503056

Tetrodotoxin, fungal pathogen infection, and bacterial microbiome associations are variable in the skin microecosystems of two *Taricha* newt species

Talon Jost [1,2*], Alysha Henderson [3], Brandon LaBumbard [4], Krisztian Magori [1], Amber Stokes [5], Danica Bergin [5], Autumn Holley [1,6], Molly Bletz [2,4], Obed Hernández-Gómez [7], Gary Bucciarelli [8], Douglas C. Woodhams [4], Jonah Piovia-Scott [3] and Jenifer B. Walke [1]

[1]Department of Biology, Eastern Washington University, Cheney, WA, United States, [2]Department of Ecosystem Science and Management, Pennsylvania State University, State College, PA, United States, [3]School of Biological Sciences, Washington State University, Vancouver, WA, United States, [4]Department of Biology, University of Massachusetts Boston, Boston, MA, United States, [5]Department of Biology, California State University Bakersfield, Bakersfield, CA, United States, [6]School of Natural Resources, University of Tennessee Knoxville, Knoxville, TN, United States, [7]Department of Fish, Wildlife and Conservation Ecology, New Mexico State University, Las Cruces, NM, United States, [8]Department of Natural Resources, University of California, Davis, Davis, CA, United States

A diverse metabolome exists on amphibian skin that mediates interactions between hosts and skin microbiomes. Tetrodotoxin is one such metabolite that occurs across a variety of taxa, and is particularly well studied in newts of the genus *Taricha* that are susceptible to infection with chytrid fungi. The interaction of tetrodotoxin with the skin microbiome, including pathogenic fungi, is not well understood, and here we describe these patterns across 12 populations of *Taricha granulosa* and *T. torosa* in Washington, Oregon, and California. We found no correlation of TTX and *Batrachochytrium dendrobatidis* (Bd) infection in either *T. granulosa* or *T. torosa*, a pattern inconsistent with a previous study. In addition, TTX, but not Bd, was significantly correlated with the skin microbiome composition in *T. granulosa*. In *T. torosa*, however, Bd, but not TTX, was correlated with the skin microbiome structure. The relationship between TTX and skin microbiome composition differed between species, with significant correlations observed only in *T. granulosa*, which exhibited higher TTX concentrations. We also detected significantly higher abundances of bacterial taxa (e.g., Pseudomonadaceae) associated with TTX production in newts with higher skin TTX. These taxa (ASVs matching *Aeromonas, Pseudomonas, Shewanella*, and *Sphingopyxis*) were associated with all body sites of previously

sampled *T. granulosa*, but not found in soil samples. Our results suggest that toxins can shape the newt skin microbiome and may influence pathogen infection through indirect mechanisms, as TTX showed no direct inhibition of Bd or *B. salamandrivorans* growth.

KEYWORDS

***Batrachochytrium dendrobatidis*, *Batrachochytrium salamandrivorans*, chytridiomycosis, disease ecology, microbial ecology, TTX, symbiosis, coevolution**

1 Introduction

The collection of symbiotic microorganisms on hosts, the microbiome, is widely recognized to play a crucial role in host health and survival (Hernández-Gómez et al., 2020; Rebollar et al., 2020), resulting in a relationship wherein hosts and symbionts respond to stressors as a single evolutionary unit (Zilber-Rosenberg et al., 2007). This coevolution with microbial symbionts can lead to highly specialized lifestyles, such as sanguivory in Vampire Bats (family Desmodontinae; Zepeda Mendoza et al., 2018) and phenolic toxin degradation in Desert Woodrats, *Neotoma lepida* (Kohl and Dearing, 2016). The amalgamation of the host's genome and the collection of microbial symbionts' genomes can be considered a single evolutionary unit, known as the holobiome (Zilber-Rosenberg et al., 2007; Theis et al., 2016).

Pathogens are among the many stressors to which hosts and their microbiomes must respond. Important advances in our understanding of interactions between pathogens and microbiomes have arisen from research on amphibians, with amphibian bacterial microbiomes playing a key role in defense against the chytrid fungal pathogens associated with numerous amphibian population declines, *Batrachochytrium dendrobatidis* (Bd) and *B. salamandrivorans* (Bsal) (Berger et al., 1998; Martel et al., 2013; Yap et al., 2017; Scheele et al., 2019; Li et al., 2021; Sewell et al., 2021; Thumsová et al., 2021). Several studies have linked susceptibility to chytridiomycosis (i.e., the skin disease caused by Bd and Bsal) to microbiome structure (Jani and Briggs, 2014; Rebollar et al., 2020; Jiménez et al., 2022). Bacterial microbiomes are known to provide defense against pathogens through the use of secondary metabolites such as violacien produced by *Janthinobacterium lividum*, which has been shown to inhibit the growth of Bd *in vitro* (Harris et al., 2009; Woodhams et al., 2014). Understanding the influence of chemical defenses that drive pathogen infection and symbiotic microbiome characteristics remains underexplored, yet valuable to understand variable disease trajectory among hosts (Longford et al., 2019).

Tetrodotoxin (TTX; $C_{11}H_{17}N_3O_8$; 319.27 Da) is an extremely potent neurotoxin found throughout many marine taxa but limited to Anura and Caudata among land vertebrates (Tsuda and Kawamura, 1952; Miyazawa and Noguchi, 2001; Moczydlowski, 2013; Lago et al., 2015). In amphibians, TTX has been associated with defense against predators (Brodie and Brodie, 1990; Brodie et al., 2005), parasites (Calhoun et al., 2017), and sympatric invasive species (Bucciarelli et al., 2023); furthermore, TTX may also have antifungal and anti-parasitic potential. Calhoun et al. (2017) and Johnson et al. (2018) found an inverse relationship between increasing TTX concentration and decreasing levels of infections with Bd, ranavirus, and parasites in both Rough-Skinned Newts (*Taricha granulosa*) and California Newts (*Taricha torosa*). However, how the symbiotic microbiome is affected by or contributes to these toxin-pathogen interactions is not known.

Prokaryotes are thought to be the primary producer of TTX, as convergent evolution of biosynthetic metabolic pathways in phylogenetically distant lineages of complex multicellular organisms for TTX manufacturing is unparsimonious and unlikely (Magarlamov et al., 2017). The biosynthesis mechanism for a single origin for TTX production and sequestration in *Taricha* newts remains inconclusive, as many laboratory experiments have been performed in respect to endogenous and exogenous origin hypotheses, producing counterintuitive results (Cardall et al., 2004; Lehman et al., 2004; Gall et al., 2012, 2022). Possession of TTX in *Taricha* newts has more recently been hypothesized to involve cutaneous microbial inhabitants (Vaelli et al., 2020). Microbial symbionts are documented to have a role in TTX production in many TTX-bearing marine organisms (Pratheepa et al., 2016; Magarlamov et al., 2017). Furthermore, amphibian skin likely selects for microbes found at a low relative abundance in the environment as members of their microbiome (Walke et al., 2014), which may permit a highly specialized relationship primed for toxin production and subsequent host utilization (Hanifin, 2010; Vaelli et al., 2020; Gall et al., 2022). Vaelli et al. (2020) isolated and cultured microbes found to produce TTX from wild-sampled *T. granulosa*, although TTX concentrations produced by these cultures were much lower than levels observed on wild individuals. Research into the dynamics of TTX production through prokaryotic symbionts and the microbial community composition dynamics, which may influence TTX production and bioavailability, remains underexplored. In addition, the role of TTX acting as a potential exaptation for pathogen and parasite remediation remains to be explored in a macroecological context.

In this field observational study, we aimed to describe the relationship between natural tetrodotoxin levels, skin microbiome

composition, and Bd infection in 12 populations of two species of *Taricha* newts. We evaluated whether these patterns were consistent between host species. We hypothesized that individuals with higher tetrodotoxin concentration would have lower Bd infection prevalence. We also hypothesized that higher tetrodotoxin concentration would influence microbiome alpha and beta diversity and that sites with high and low tetrodotoxin concentration would have commensurate levels of known TTX-producing microbes (Vaelli et al., 2020).

2 Materials and methods

2.1 Sample collection

Two *Taricha* newt species (*Taricha granulosa:* n = 90, *Taricha torosa:* n = 40) were sampled for Bd infection, skin microbiome composition, and TTX quantification from 12 distinct locations in Washington, Oregon, and California (Figure 1). Sites were selected to capture a range of TTX levels, based on previous TTX quantification by Hanifin et al. (2008). Sampling occurred in February 2020 for *T. torosa*, and between May and July 2021 for *T. granulosa*. One individual *T. granulosa* did not have a skin punch collected for TTX concentration due to emaciation and health concerns. Mass, snout to vent length (SVL), and sex were also recorded. Sampling was performed in accordance with the following approved permits: Oregon Department of Fish and Wildlife (Permit No. 092-21), Washington Department of Fish and Wildlife (Scientific Collection Permit PIOVIA-SCOTT 20-312), California Department of Fish and Wildlife (Permit No. SC-12430), Washington State University IACUC protocol (ASAF#6339), and University of California, Los Angeles IACUC (2013-011-13 C).

Each individual newt was rinsed twice for 5 seconds with sterile deionized water to reduce transient bacteria (Lauer et al., 2007), and then skin swabs were collected using rayon-tipped sterile applicators for a standard number of strokes on the skin (Roth et al., 2013). The swab was placed into an empty 2 mL microcentrifuge tube for molecular microbiome characterization and Bd infection quantification, and for *T. granulosa*, a second swab was collected and stored in 20% glycerol for culturing (culturing data are not presented in this study). Samples were stored on dry ice in the field and then transferred to a -80°C freezer within 48 hours of collection (Piovia-Scott et al., 2015).

Skin samples for TTX quantification were obtained from *T. granulosa* by anesthetizing individuals using buffered 0.1% tricaine methanesulfonate (Ethyl 3-aminobenzoate methanesulfonate salt – MS-222) and collecting a 2.5 mm radius dorsal tissue sample between the pectoral and pelvic girdle using a sterile skin biopsy tool (Hanifin et al., 2004). After sample collection, newts were rinsed with sterile water and received an antiseptic and pain-relieving solution before final release upon anesthesia revival (Downes, 1995). *Taricha torosa* were sampled for TTX quantification similarly to the methods described for *T. granulosa*, except a 2 mm radius of dorsolateral tissue was sampled from adults using a sterile skin biopsy tool (Bucciarelli et al., 2014). Tissue samples were stored in 300 µL of 0.1 M aqueous acetic acid and held on dry ice until being transferred to a -80°C freezer for later

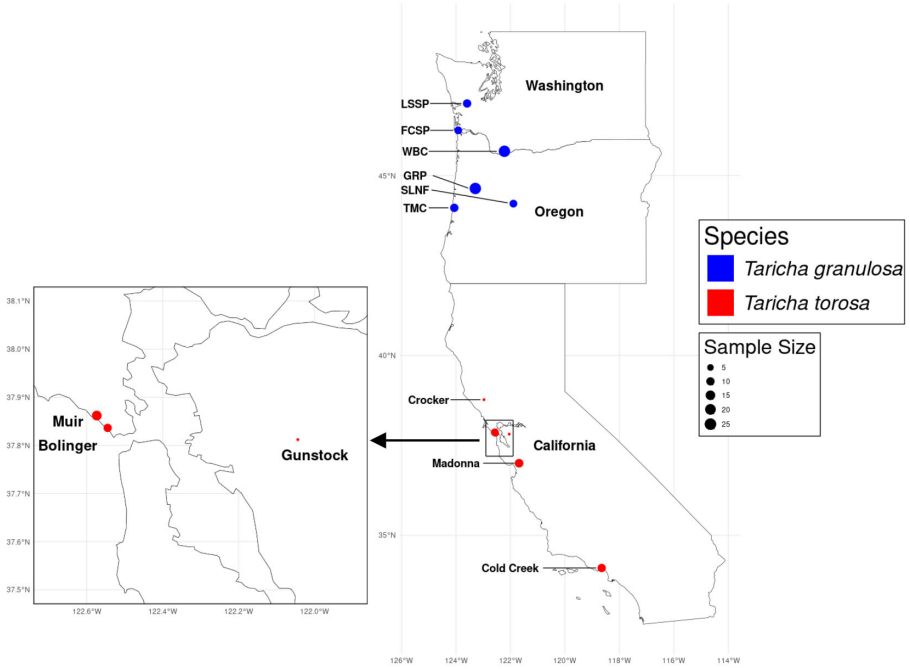

FIGURE 1
Sampling location distribution map for locations in Washington, Oregon, and California with blue dots representing *T. granulosa* sites and red dots representing *T. torosa* sites. The size of the location dot corresponds to the sample size for each site, respectively. Figure was created using the following R packages: *rnaturalearth* (https://github.com/ropensci/rnaturalearth.git) *units* (Pebesma et al., 2016), and *sf* (Pebesma and Bivand, 2023).

extraction (Buttimer et al., 2022). All the sampling tools were cleaned and sterilized between individuals and replaced between sites.

2.2 TTX quantification

Tetrodotoxin concentration was quantified for *T. granulosa* using a Competitive Inhibition Enzymatic Immunoassay (CIEIA) procedure as in Stokes et al. (2012). Standards were prepared using TTX-citrate (Abcam, Cambridge, United Kingdom) and ranged from 10-500 ng/mL. Values above 500 ng/mL were diluted in 1% PBS-BSA. No samples were below 10 ng/mL in concentration. The average interplate coefficient of variation was 6.84%. *Taricha torosa* TTX samples were quantified using a high performance liquid chromatography system coupled with fluorescence detection (HPLC-FLD) (Bucciarelli et al., 2014). It has been shown that quantification of TTX using HPLC and CIEIA techniques yield highly correlated results (Williams et al., 2016). Further, studies investigating the TTX levels of newts from the same location in Benton County, Oregon have fallen within the same range, when excluding one newt with 28 mg of TTX that doubled the mean (Stokes et al., 2015; Charles Hanifin personal communication). Although we used different methods for TTX quantification for each species, these methods are comparable to each other (Williams et al., 2016), and the levels of TTX in *T. granulosa* are generally higher than in *T. torosa* in other studies (e.g., Johnson et al., 2018). Tetrodotoxin levels of individual newts were assigned a designation of 'high' or 'low' if the estimated whole newt TTX levels were greater or less than 1 mg, using the procedure outlined in Hanifin et al. (2004) which uses a summation of estimated total skin surface area to predict whole newt TTX levels.

2.3 Molecular methods for Bd quantification and microbiome characterization

DNA extractions of microbiome skin swabs for *T. granulosa* and *T. torosa* were performed using a Qiagen DNeasy Blood and Tissue Kit (Qiagen, Hilden, Germany) according to the manufacturer's protocols for Gram positive bacteria. This included an initial lysozyme incubation step that was conducted by adding 180 µL of a lysozyme buffer (20 mg lysozyme/mL lysis buffer) to each swab sample and incubating at 37°C for 30 minutes. Next, 25 µL proteinase K and 200 µL Buffer AL were added to each sample and incubated at 70°C for 30 minutes. The extracted DNA was used to quantify Bd infection intensity (in ITS gene copy numbers) and characterize skin bacterial communities.

Bd infection intensity was quantified using real-time TaqMan quantitative Polymerase Chain Reaction (qPCR) on the Bio-Rad CFX96 Touch Real-Time PC Detection System following the protocol established in Boyle et al. (2004). Reactions for newt samples were performed in duplicate in 96-well plates with three negative controls containing RNA-spiked water. If detection differed between the duplicate reactions, a third reaction was conducted for verification. Bd infection intensity estimates were determined for each sample using a linear standard curve generated by gBlock ITS (Integrated DNA Technologies, Coralville, Iowa) serial dilutions of 10^6 through 10^1 performed in triplicate (while standard curve for *T. granulosa* samples were 10^3 through 10^0 ITS gene copies). Duplicate samples were then averaged and estimated ITS gene copy numbers (i.e., Bd infection intensity) were generated for each individual for analysis.

Newt skin bacterial community composition was characterized using amplicon sequencing of the V4-V5 region of the 16S rRNA gene with primers 515F (barcoded) and 926R for *T. granulosa*, and the V4 region of the 16S rRNA gene with primers 515F (barcoded) and 806R for *T. torosa* (Caporaso et al., 2011, 2012; Quince et al., 2011; Parada et al., 2016). While different reverse primers were used, a previous study found little difference between clustering pattern and relative abundance when comparing the primers (Walters et al., 2015). For *T. granulosa*, triplicate reactions per sample were performed, with each reaction containing 12 µL Qiagen UltraClean PCR-grade H_2O (Qiagen, Hilden, Germany), 10 µL Quantabio AccuStart™ II PCR SuperMix (Quantabio, Beverly, United States), 0.5 µL Illumina Forward primer/barcode 515F (Illumina, San Diego, United States), 0.5 µL Illumina Reverse primer 926R (Illumina, San Diego, United States), and 2 µL sample DNA. Reactions were processed on a Bio-Rad T100™ Thermal Cycler (Bio-Rad Laboratories, Hercules, United States) for 25 µL samples under the following conditions: 1) 94°C for 3 minutes, 2) 94°C for 45 seconds to denature the DNA, 3) 50°C for one minute to anneal primers to the DNA, 4) 72°C for 1.5 minutes to elongate the DNA, 5) Steps 2 to 4 were repeated for 35 cycles, 6) 72°C for 10 minutes, and 7) 4°C hold. Amplicons from triplicate PCR reactions were pooled and analyzed using 1% agarose gel electrophoresis stained with Thermo Fisher™ GreenGlo DNA safe stain (Thermo Fisher Scientific, Waltham, MA, United States) and 1% Tris-Borate-EDTA (TBE). Each sample had an associated negative no-template control used to confirm lack of contamination in reagents. Samples were quantitated using a Qubit™ 4.0 fluorometer (Invitrogen, Carlsbad, CA, United States), then pooled at equimolar concentrations. A Qiagen QIAquick PCR Purification Kit (Qiagen, Hilden, Germany) was used to clean the pooled, multiplexed samples prior to amplicon sequencing. Multiplexed samples were sequenced using Illumina MiSeq (250bp single-end) at the Dana Farber Cancer Institute at Harvard University. For *T. torosa*, duplicate reactions per sample were performed, with each reaction containing 9.5 µL Millipore Milli-Q water, 12.5 µL Azura 2x HS Taq Red Mix (Azura Genomics, Raynham, MA, United States), 0.5 µL of each primer, and 2 µL sample DNA. Reactions were processed on a Eppendorf Mastercycler Nexus Thermal Cycler (Eppendorf, Hamburg, Germany) using the following conditions: 1) 95°C for 2 minutes, 2) 28 cycles of 95°C for 15 seconds, 50°C for 45 seconds, and 72°C for 90 seconds, 3) 72°C for 10 minutes, and 4) 10°C hold. Amplicons from duplicate reactions were pooled and visualized on a 1.5% agarose gel and then purified and normalized using a Mag-Bind EquiPure Library Normalization Kit (Omega Bio-tek, Norcross, GA, United States). After normalizing, all samples were pooled for library preparation, and the library was quantitated using a QubitTM 4.0 fluorometer (Invitrogen, Carlsbad,

CA, United States) and sequenced at the University of Massachusetts, Boston in the Biology Department using an Illumina MiSeq v2 cartridge (300bp single-end, trimmed to 250bp). Sequences were deposited in the NCBI SRA database under Project SUB14754928.

2.4 Microbiome analysis

Newt microbiome sequencing data from each species were processed separately to tailor the filtering parameters and rarefaction depth for the quality and quantity of each species' sequences. The datasets were then combined to investigate species differences in microbiomes. Because the two newt species had significantly different microbiomes (see Results section), all remaining microbiome analyses were performed on each newt species' dataset separately.

For *T. granulosa*, Quantitative Insights Into Microbial Ecology 2 (QIIME2; v.2023.7; Bolyen et al., 2019) was used with a workflow similar to that in Walke et al. (2015). Samples (n = 89) were checked for quality score using visual plots created by FastQC (v.0.12.1. http://www.bioinformatics.babraham.ac.uk/projects/fastqc/) and visualized with MultiQC (v.1.19: Ewels et al., 2016). Trimmomatic (v.0.39; Bolger et al., 2014) was used to trim sequences with a quality score less than 20 using a sliding window of 5 to 20 with reads less than a 90 minimum length dropped (Bolger et al., 2014). Sequences were imported into QIIME2 and filtered by quality using *quality-filter q-score* to filter sequences potentially missed by Trimmomatic (Bokulich et al., 2013). After quality filtering, 89 samples containing 9,938,507 total reads were imported (reads per sample ranged from 6 to 926,070). Samples were processed using *deblur* (https://github.com/biocore/deblur) to correct sequencing errors by clustering into amplicon sequence variants (ASVs) with a 0.005% mean error threshold and 20 read minimum, retaining 88 samples with 984 ASVs (total reads = 1,042,089; reads per sample ranged from 1,135 to 164,401).

Taricha torosa samples (n = 42) were processed similarly using QIIME2 (v.2021.4). Samples were quality filtered and demultiplexed with a total of 916,197 reads generated, and then processed with *deblur* to further quality filter and cluster reads into ASVs with a 0.005% mean error threshold and 20 read minimum, retaining 40 samples (38 newts, a PCR control, and an extraction control) with 828 ASVs (total reads = 357,000; reads per newt sample ranged from 4,246 to 13,775).

Taxonomy was assigned to the sequences using a *sklearn* naïve Bayes taxonomic classifier (Pedregosa et al., 2011) trained with the Silva 138 SSU Ref NR 99 (Quast et al., 2012; https://www.arb-silva.de/documentation/release-138/). A multiple sequence alignment was conducted using MAFFT (v.7.525; Katoh et al., 2002), and a 16S rRNA phylogenetic tree (rooted and unrooted) was created using IQ-TREE (v2.3.4; Nguyen et al., 2015). The *deblur* feature table was filtered using *q2-taxa* to remove ASVs designated mitochondria, chloroplast, unassigned, and Archaea. For the *T. granulosa* dataset, infrequently observed ASVs were identified through integration of the *decontam* plugin (Davis et al., 2018) using *quality-control decontam-identify* and removed with a threshold of 0.1 using *quality-control decontam-remove*, removing a total of 874 contaminant reads and 13 contaminant ASVs. The resulting dataset contained 88 samples with 882 ASVs and 1,022,255 total reads. As for the *T. torosa* dataset, ASVs found in the extraction and PCR controls with greater than 20 reads were removed as contaminants, resulting in 15 ASVs being removed resulting in a total of 813 ASVs and 351,423 total reads.

Samples were rarefied at 2,200 (*T. granulosa*) and 3,800 (*T. torosa*) sequences per sample to obtain an equal number of sequences per sample for each species. Rarefaction depth was chosen based on evaluation of alpha rarefaction plots for plateauing levels of diversity with sequencing depth. Samples with fewer reads than the rarefied depth were dropped, retaining 83 (93.25%) of the original 89 *T. granulosa* samples (875 ASVs and 182,600 reads) and 34 (87.18%) of the original 39 *T. torosa* samples (744 ASVs and 133,000 reads). QIIME2 was used to calculate ASV frequencies per sample, alpha diversity (Shannon's diversity index, Faith's Phylogenetic Diversity, observed ASVs, and Pielou's evenness), beta diversity (Jaccard similarity, Bray-Curtis dissimilarity, unweighted UniFrac distance, and weighted UniFrac distance), and Principal Coordinates Analysis (PCoA). Two additional samples were excluded from analyses due to only a single individual being sampled at a site, resulting in 32 samples being retained. Data was exported to Rstudio (2023.1: R v.4.3.3. R Core Team, 2023) for further analysis.

To identify if any of our Illumina sequences matched sequences of bacteria known to produce TTX (Vaelli et al., 2020; Dryad Dataset), we compared the representative sequences of the rarefied ASV tables for both newt species using *vsearch* (Rognes et al., 2016) with a 99% identity threshold. We obtained the total reads associated with known TTX-producing microbes, the total proportion of sample reads associated with known TTX producing microbes, and the overall richness of TTX-producing ASVs found in our dataset. We also compared the ASV tables to TTX concentration to find taxa enriched in high TTX microenvironments using an Analysis of Compositions of Microbiomes with Bias Correction (see below). Similarly, we predicted the proportion of TTX producing bacteria for microbiome data from Vaelli et al. (2020), including skin regions, cloacal, and soil samples using custom scripts that match known TTX producing bacteria to the next generation sequence reads based on 99% sequence similarity in the 16S gene.

2.5 TTX activity against growth of *Batrachochytrium* fungi

Growth inhibition assays were performed to assess if TTX could inhibit the growth of both Bd and Bsal with a dose-response curve analysis. One mg of TTX was dissolved in 1 mL of Millipore Milli-Q water and then sterilized by passing the solution through a 0.22 µm filter. Dilutions were made to test growth inhibition at the following concentrations: 250, 100, 50, 45, 40, 35, 30, 25, 20, and 15 µM. Each concentration was tested in triplicate against Bd (JEL 423) or Bsal (AMFP13/1) by performing a 96-well growth inhibition assay after Bell et al. (2013). Bd was grown on 1% tryptone and Bsal on TGhL agar plates until motile zoospores were released by mature

sporangia. Zoospores were harvested by incubating plates with 3 mL 1% tryptone (Bd) or TGhL (Bsal) liquid media for 15 minutes and then normalizing to a concentration of 2×10^6 zoospores/mL. Sample test wells contained 50 µL of Bd or Bsal zoospore solution and 50 µL of the appropriate TTX solution. Positive controls contained 50 µL of zoospore solution and 50 µL of 1% tryptone media for Bd, or TGhL media for Bsal. Two negative controls were added, where one contained 100 µL of appropriate media (as a media blank control to check for assay contamination), and a heat-killed control contained 50 µL of heat-killed zoospore solution (incubated at 60°C for 30 minutes) and 50 µL of the appropriate media. All reactions were set up in six replicates. Growth was measured as optical density at 492 nm on a spectrophotometer on days 0, 3, 5, and 7 for Bd incubated at 19°C, and days 0, 3, 5, 7, and 9 for Bsal at 15°C.

2.6 Statistical analysis

Since our datasets for *T. granulosa* and *T. torosa* were collected separately and in different locations, each dataset was analyzed independently. To assess whether TTX concentration varied among locations and between both sexes and species, we used a Kruskal-Wallis test. To address multiple comparisons concerning location, a Dunn's *post-hoc* test with a Bonferroni correction was applied to find significant differences. To assess whether Bd infection intensity and prevalence varied among locations and between sexes and species we used a Kruskal-Wallis test, and for multiple comparisons of location we used a Dunn's *post-hoc* test with a Bonferroni correction. For analyses investigating Bd infection intensity and intensity across location, only sites with three or more Bd positive individuals were included to meet sample size requirements for statistical validity.

We used Generalized Linear Mixed Models (GLMMs) with a binomial error distribution and a log link function to investigate the effect of TTX on Bd infection status for the overall species datasets and, in a separate set of analyses, Bd positive locations only. The response variable was Bd infection status and the predictor variables were TTX concentration and location; to account for non-independence of individuals from the same location, we used location as a random effect variable in all of our models. To test the significance of predictor variables within the proposed models we used Likelihood Ratio tests. To investigate the association of TTX as a response variable and microbiome alpha diversity as a predictor variable, we used Linear Mixed Models (LMMs) with location as a random variable. We used F-tests with denominator degrees of freedom estimated using Satterthwaite approximations to test for the significance of the model. We also investigated alpha diversity as a function of Bd infection intensity for all samples, Bd positive locations, and Bd positive individuals using LMMs with location as a random effect. We used linear regressions to investigate associations between putative TTX-producing ASVs and TTX concentration using individual ASVs and the relative abundance of all matching putative TTX ASVs as a single predictor for each species.

To decide whether the microbiomes of *T. granulosa* and *T. torosa* would be analyzed together as a single dataset or kept separate for analyses, a Permutational Analysis of Variance (PERMANOVA) was conducted within QIIME2 using beta diversity matrices to examine if there was a significant difference in microbiome structure between species. PERMANOVAs were conducted within QIIME2 with beta diversity matrices as the independent variable to examine similarity and dissimilarity with respect to categorical variables (TTX high/low, Bd infection presence/absence, location, sex). For continuous variables (TTX concentration, Bd infection intensity, mass), Mantel tests were conducted on beta diversity matrices within QIIME2 using the *diversity beta-correlation* function. We conducted PCoA on QIIME2-derived Bray-Curtis matrices for both species using the *ggords* (V1.18: Beck, 2017) and *qiime2R* (V0.99.20: Bisanz, 2018) packages and subsequently created ordination plots to visualize clustering among samples. An Analysis of Compositions of Microbiomes with Bias Correction (ANCOM-BC; Lin and Peddada, 2020) was performed on the rarefied samples in respect to the TTX high classification to assess potential influential community members and their relative enrichment or depreciation in the system using the *ancombc2* package (Lin and Peddada, 2020). We characterized the core microbiome for both species using post-rarefaction tables and considered any taxa present in 70% of individuals for a given species and collectively represented 75% of the total frequency to be a core microbiome member (Custer et al., 2023; Yu et al., 2023).

Percent growth of Bd and Bsal in the presence of various TTX concentrations was calculated by 1) taking the slope of the optical density over the incubation days, 2) subtracting the averaged slope of the heat-killed negative controls from the slope of each sample and positive control, 3) dividing the corrected sample slopes by the averaged slope of the corrected positive controls, and 4) multiplying by 100 to get percent growth. Differences in Bd or Bsal percent growth between multiple TTX concentrations and positive controls was determined using a one-way ANOVA and Dunnett's *post-hoc* test.

3 Results

3.1 Tetrodotoxin concentrations

Mean TTX concentration was greater in *T. granulosa* than *T. torosa* ($\chi^2 = 8.76$, $p = 0.003$). TTX concentration for *T. granulosa* individuals ranged from 0.061 mg to 6.718 mg, with a mean of 1.94 mg and standard deviation of ± 2.24 (males: mean ± SD = 2.26 ± 2.36; females: mean ± SD = 1.25 ± 1.78), and was significantly different among locations ($\chi^2 = 63.405$, $p < 0.0001$; Figure 2). For *T. granulosa*, there were more males than females in our samples (males: n = 61, females: n = 29), but TTX concentration was not significantly different between newt sexes ($\chi^2 = 2.61$, $p = 0.11$). TTX concentration for *T. torosa* ranged from 0.0025 mg to 1.83 mg, with a mean of 0.47 mg and a standard deviation of ± 0.46 (males: mean ± SD = 0.42 ± 037; females: mean ± SD = 0.58 ± 0.63), and was significantly different

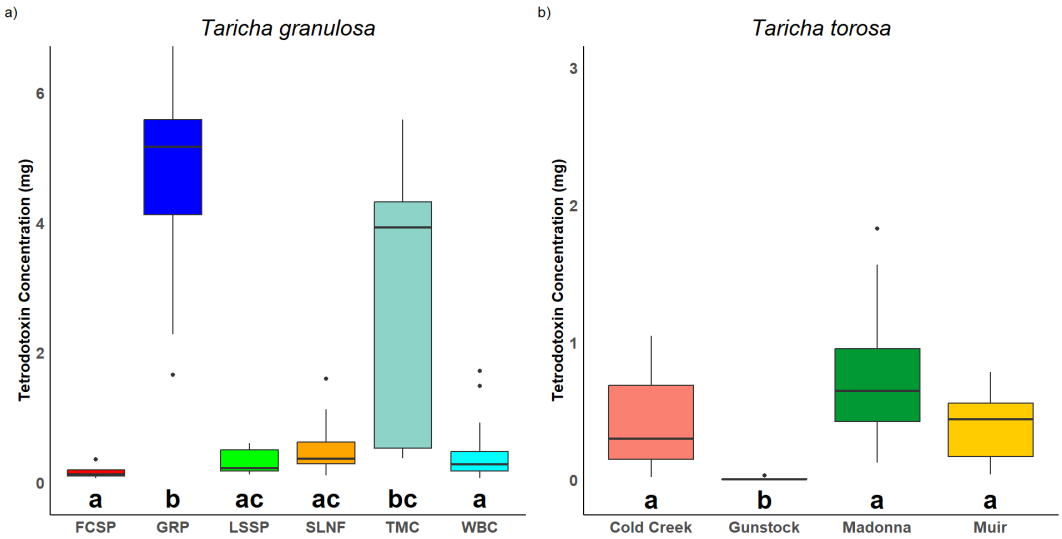

FIGURE 2
Tetrodotoxin concentration by location for **(A)** *T. granulosa* and **(B)** *T. torosa*. Sites in Washington, USA include GRP, TMC, and SLNF. Sites in Oregon, USA include FCSP, LSSP, and WBC. Sites in California, USA include Cold Creek, Gunstock, Madonna, and Muir. Horizontal black lines represent median values. Letters below boxplots represent Dunn's *post-hoc* test results where locations which are not significantly different from each other will contain matching letters while locations that are significantly different will not have matching letters. Letters in the plot of one species are unique to that species and do not correspond to the other plot. Points above the boxplots which fell outside the 1.5 times interquartile range of the plots were presented as dots.

among locations (χ^2 = 17.56, p < 0.001; Figure 2). For *T. torosa*, there were also more males than females in our samples (males: n = 26, females: n = 11), and TTX concentration was not significantly different between sexes (χ^2 = 0.009, p = 0.92).

3.2 *Batrachochytrium dendrobatidis* infection patterns

Batrachochytrium dendrobatidis prevalence was 40.9% overall (51/127 total individuals; *T. granulosa* = 37/90, 41%; *T. torosa* = 15/37, 40.54%). Bd infection was present at 70% of sampled locations (7/10 locations overall, *T. granulosa* = 5/6, *T. torosa* = 2/4), although one of the five Bd-positive sites for *T. granulosa* had only one positive individual. Among infected individuals, Bd infection intensity ranged from 45.8 to 23,038.6 ITS copies, with a mean of 2,105.8 ITS copies and standard error of ± 565 (*T. granulosa*: mean ITS copies ± SD = 1738.3 ± 2899.3: Figure 3A; *T. torosa*: mean ITS copies = 1.14 ± 4107.9. Figure 3B). There were no differences in Bd infection intensity or status between newt species (all samples included: status: χ^2 = 0.004, p = 0.95, intensity: χ^2 = 0.26, p = 0.61; Bd-positive samples only: intensity: χ^2 = 2.33, p = 0.13). Bd infection status was not significantly different between newt sexes for either species when accounting for differences in location (*T. granulosa:* df = 1, Coef = -0.31, χ^2 = 0.38, p = 0.54; *T. torosa*: df = 1, Coef = 2.96, χ^2 = 1.23, p = 0.27). Bd infection intensity and status were significantly different among locations for both species when all individuals were included (*T. granulosa*: intensity: χ^2 = 14.61, p = 0.01, status χ^2 = 17.05, p < 0.01: Figure 3C; *T. torosa*: intensity: χ^2 = 27.81, p < 0.0001; status: χ^2 = 27.81, p < 0.001. Figure 3D). Bd infection intensity was still significantly different among locations when only locations with confirmed Bd infection were included for *T. torosa* (χ^2 = 7.04, p < 0.01), but not *T. granulosa* (χ^2 = 7.81, p = 0.10). Similarly, when only individuals with confirmed Bd infection were included, Bd infection intensity was significantly different among sites for *T. torosa* (χ^2 = 27.81, p < 0.0001), but not *T. granulosa* (χ^2 = 6.10, p = 0.19). Bd infection status was significantly different among locations with confirmed Bd infection for both species (*T. granulosa*: χ^2 = 9.89, p = 0.04; *T. torosa*: χ^2 = 6.60, p = 0.01).

3.3 Relationship between tetrodotoxin and Bd infection

Bd infection status was not significantly associated with TTX concentration for either newt species when all individuals were included (*T. granulosa*: df = 1, Coef = 0.24, χ^2 = 2.16, p = 0.14; *T. torosa*: df = 1, Coef = 0.07, χ^2 = 0.0004, p = 0.98 Figure 4), nor when only Bd positive locations were included (*T. granulosa*: df = 6, Coef = 0.17, χ^2 = 1.42 p = 0.23; *T. torosa*: df = 1, Coef = 0.20, χ^2 = 0.07, p = 0.94).

3.4 Skin microbiome composition and diversity

The two *Taricha* newt species had significantly different microbiome structure and composition (Figure 5; PERMANOVA on Weighted-Unifrac: Pseudo-f = 12.59, p = 0.001); thus, further microbiome analyses were conducted separately for each newt species. The most abundant taxa for *T. granulosa* species were

10.3389/famrs.2024.1503056

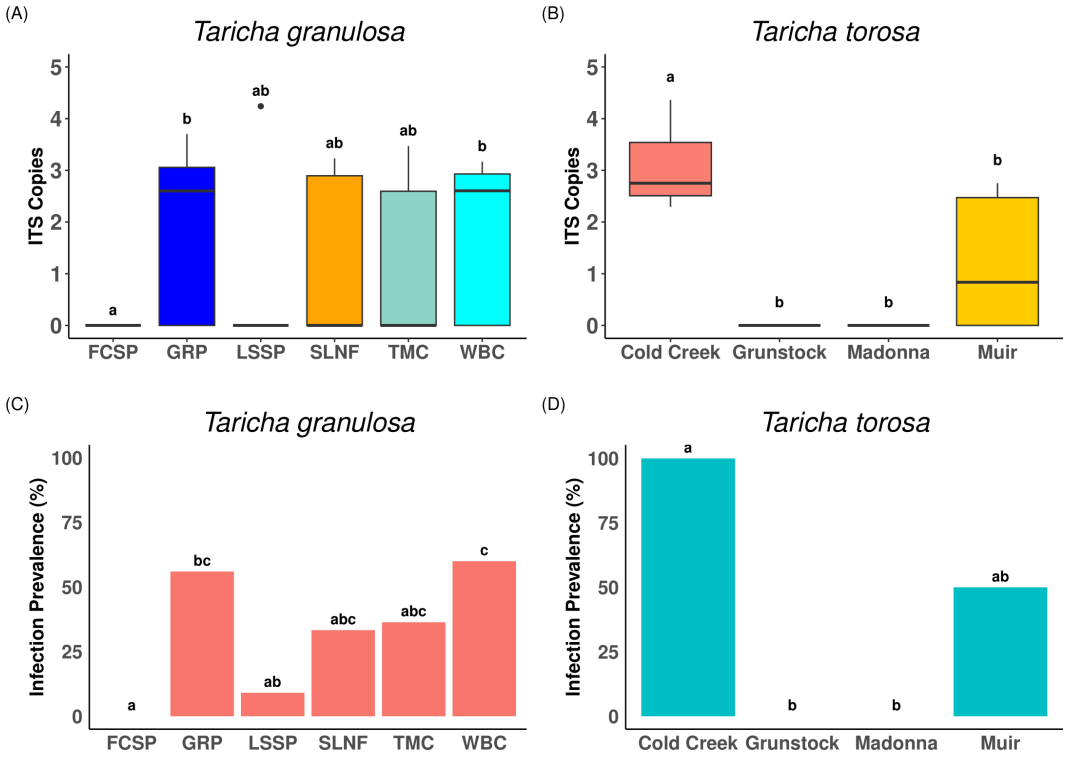

FIGURE 3
Bd infection intensity and prevalence for *T. granulosa* and *T. torosa*. Bd infection intensity using Log10 + 1 transformed ITS gene copy number by location for **(A)** *T. granulosa* and **(B)** *T. torosa*. Bd infection prevalence (% of Bd positive samples at that location) for **(C)** *T. granulosa* and **(D)** *T. torosa*. Horizontal black lines represent median values. Letters above boxplots and barplots represent Dunn's *post-hoc* test results where locations which are not significantly different from each other will contain matching letters while locations that are significantly different will not have matching letters. Letters on the top of the plot of one species are unique to that species and do not correspond to the other plot.

Gammaproteobacteria (48.6%), Bacteroidia (24.9%), and Alphaproteobacteria (13.3%), while the most abundant taxa for *T. torosa* were Gammaproteobacteria (61.6%), Bacilli (20.5%), and Bacteroidia (12.3%) (Figure 5). Five ASVs were identified as core members for *T. granulosa*, but no core ASVs were identified for *T. torosa* (Table 1).

Skin microbiome alpha diversity for both *T. granulosa* and *T. torosa* were significantly different across sites, with the exception of Pielou's evenness in *T. torosa*, which was borderline significantly different across sites (Table 2). Alpha diversity was not significantly different between Bd infected and uninfected newts for either species, nor was Bd infection intensity correlated with alpha diversity (Table 2). For TTX levels (high/low), alpha diversity was not different between levels, and this pattern was the same in both newt species (Table 2). For TTX concentration, no alpha diversity metrics were correlated with TTX in *T. granulosa*, but ASV richness and Faith's Phylogenetic Diversity were negatively correlated with TTX in *T. torosa* (Table 2). The ANCOM test identified six ASVs which had an enriched relative abundance in high TTX *T. granulosa*, but found no microbes that were enriched or depreciated for *T. torosa* (Figure 6). Female newts had higher Faith's Phylogenetic Diversity than males for both *T. granulosa* and *T. torosa* (Table 2). Mass was not correlated with alpha diversity for either newt species (Table 2).

Newts sampled from different locations had significantly different microbiome structure; this was the case for both newt species and for all beta diversity metrics (Figures 7A, D; Table 3). No newt skin microbiome structures were correlated with TTX concentrations in either species (Figures 7B, E; Table 3); however skin microbiome structure was correlated with TTX concentration classified as high and low for *T. granulosa*, but not *T. torosa* (Table 3). On the other hand, newt skin microbiome structure was correlated with Bd infection intensity in *T. torosa*, but not in *T. granulosa* (Figures 7C, F; Table 3). *T. torosa* newts also had significantly different microbiomes depending on Bd infection status (present/absent) (Table 3). Male and female newts had similar microbiome structure in both species, and lastly, body mass was correlated with at least one beta diversity metric in both species (Table 3).

3.5 Microbiome comparison to dataset of known TTX-producing bacteria

Matching our Illumina sequences to the Vaelli et al. (2020) dataset of TTX-producing bacteria identified four *Pseudomonas* spp. found on *T. granulosa*, and three *Pseudomonas* spp., one *Aeromonas* sp., and one *Shewanella* sp. found on *T. torosa* (Table 4). These putative TTX-producing bacteria represent an overall relative abundance of 6.05% and 1.32% on *T. granulosa* and *T. torosa*, respectively. TTX concentration in *T. granulosa* was negatively correlated with the relative abundance of putative

10.3389/famrs.2024.1503056

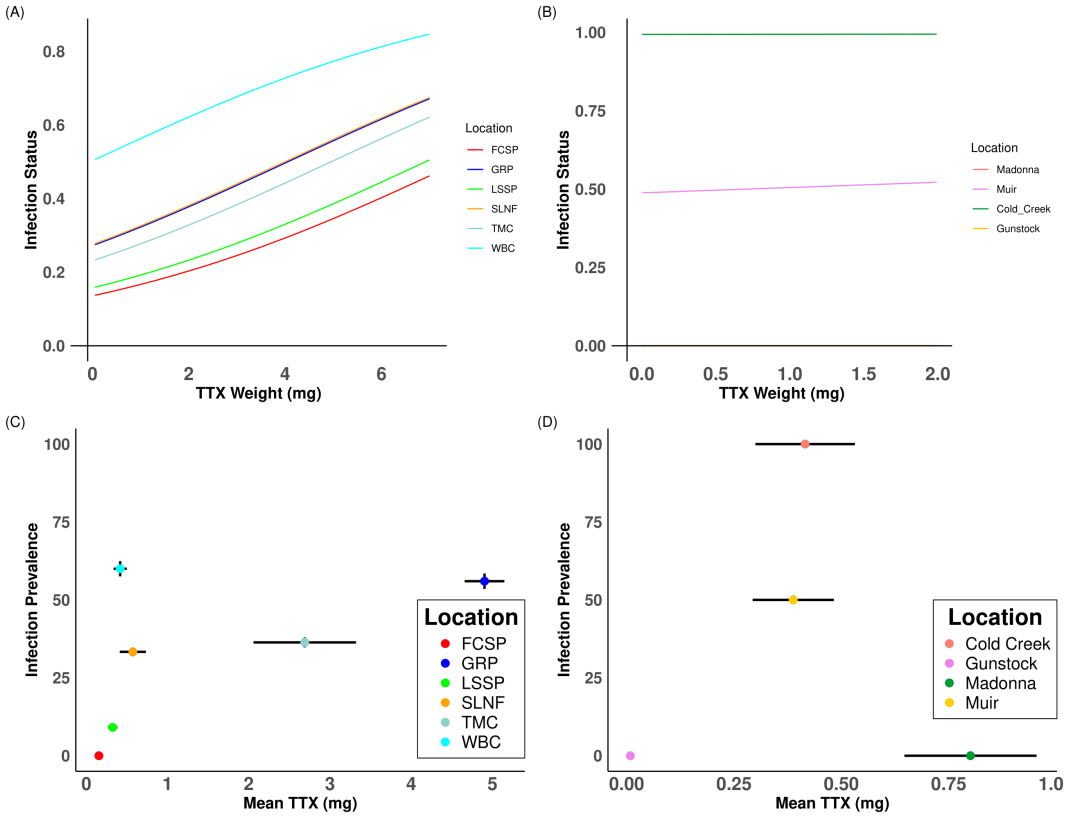

FIGURE 4
General Linear Mixed Model with location as a random effects variable showing increasing tetrodotoxin concentration on the x-axis and the effect (weight) of tetrodotoxin concentration on infection status on the y-axis for **(A)** *T. granulosa* and **(B)** *T. torosa*. Infection prevalence for each location plotted against mean tetrodotoxin concentration for **(C)** *T. granulosa* and **(D)** *T. torosa*. Horizontal error bars represent the standard deviations for tetrodotoxin concentration respective of that location. Vertical error bars represent the standard deviation of infection prevalence respective of that location.

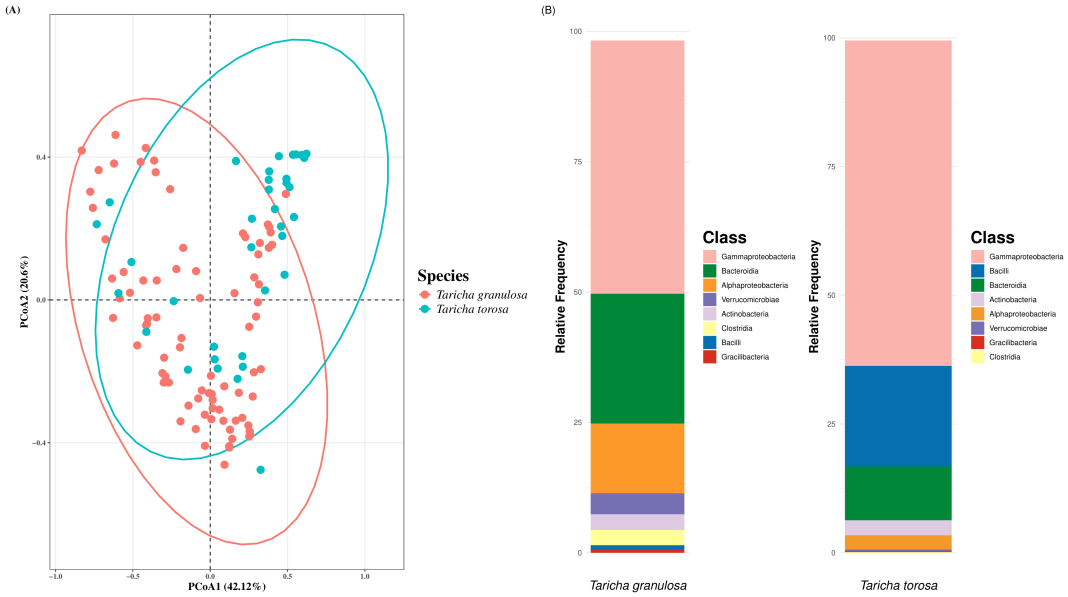

FIGURE 5
(A) PCoA ordination plot using QIIME2-derived weighted-UniFrac distance matrices for *T. granulosa* (red) and *T. torosa* (blue). **(B)** Taxonomic barplot showing relative frequency of the top 8 classes within the microbiomes of *T. granulosa* (left) and *T. torosa* (right).

TABLE 1 Core microbiome for *T. granulosa* computed using QIIME 2 feature-table core-features with an ASV kept if present in 70 percent of sample microbiomes (n = 89).

	Order	Family	Genus	Species	Prevalance (%)	Mean relative abundance (%)
Taricha granulosa	Burkholderiales	Comamonadaceae	NA	NA	66.3	13.6
	Xanthomonadales	Xanthomonadaceae	*Stenotrophomonas*	*rhizophila*	67.4	5.9
	Burkholderiales	Neisseriaceae	*Uruburuella*	*sp.*	79.8	4.1
	Rhizobiales	Devosiaceae	*Devosia*	*sp.*	66.3	1.2
	Xanthomonadales	Xanthomonadaceae	*Stenotrophomonas*	*rhizophila*	71.9	0.9

No core ASVs were identified for *T. torosa*.

TTX-producing bacteria (t-value = - 2.85, $p < 0.01$), but was not significantly correlated with the richness of TTX-producing ASVs (t-value = -1.44, p = 0.15). For the four matching *Pseudomonas* ASVs, only one exhibited a negative correlation with TTX concentration (TX174011: Coef = -0.06, t-value = -2.47, p = 0.02), while the other three matches exhibited no correlation with TTX concentration (Table 5). In *T. torosa*, TTX concentration was not significantly correlated with either relative abundance of putative TTX-producing bacteria (t-value = -0.52 p = 0.61) or number of TTX-producing ASVs, richness (t-value = -0.49, p = 0.62). For the six matching ASVs, none exhibited a significant correlation with TTX concentration (Table 5).

Overall, there were low levels of predicted TTX-producing bacteria in the microbiomes from Vaelli et al. (2020) samples (Supplementary Figure S1). The soil samples had nearly no predicted TTX-producing bacteria compared to that of *Taricha* body site samples.

3.6 TTX activity against growth of *Batrachochytrium* fungi

TTX did not inhibit the growth of Bd ($F_{10,41} = 1.248$; P = 0.291) nor Bsal ($F_{10,41} = 1.807$; P = 0.090) in the growth inhibition assays. From the Dunnett's *Post Hoc* test, no concentration of TTX significantly affected the growth of Bd and Bsal (Supplementary Figure S2; Supplementary Table S2).

4 Discussion

Tetrodotoxin (TTX)-bearing terrestrial animals, such as *Taricha* newts, have long been studied in the context of a coevolutionary arms race with their predators, as TTX appears to play a role in western newts' predation defense (Brodie et al., 2002, 2005; Williams et al., 2012; Reimche et al., 2020) and mating (Frey

TABLE 2 Generalized Linear Mixed Models (GLMMs) of the numeric alpha diversity metric obtained from QIIME2 diversity-core metrics as a response variable against the categorical predictor variables Bd infection presence/absence, and sex with Likelihood Ratio test (LR) to assess the model with the variable; and Linear Mixed Models (LMMs) of numeric alpha diversity metrics against predictor variables: tetrodotoxin high/low classification, tetrodotoxin (mg), Bd infection intensity, and mass tested using F-tests with denominator degree of freedom adjustments using Sattrthwaite's method. Kruskal-Wallis test of alpha diversity variables as response variables against location as a predictor variable.

Category	*Taricha granulosa*				*Taricha torosa*			
	ASVs	Shannon's	Faith's	Evenness	ASVs	Shannon's	Faith's	Evenness
TTX (High/Low)	0.48	0.95	0.17	0.64	0.38	0.94	0.47	0.69
TTX (mg)	0.87	0.97	0.36	0.97	**0.04**	0.4	**0.02**	0.91
Bd (Presence/Absence)	0.91	0.38	0.72	0.2	0.43	0.9	0.37	0.91
Bd infection Intensity (All Samples)	0.91	0.33	0.66	0.18	0.61	0.79	0.73	0.65
Bd infection Intensity (Bd Positive Locations)	0.78	0.27	0.58	0.15	0.06	0.92	0.33	0.58
Bd infection Intensity (Bd Positive Individuals)	0.41	0.8	0.59	0.3	0.48	0.46	0.99	0.19
Location	**< 0.0001**	**< 0.0001**	**< 0.0001**	**0.001**	**0.01**	**0.001**	**0.01**	**0.05**
Sex	0.06	0.26	**0.047**	0.64	0.21	**0.04**	0.21	0.07
Mass	0.57	0.6	0.62	0.56	0.15	0.09	0.07	0.22

P-value for each test is provided.
Bold values indicate significance p > 0.05.

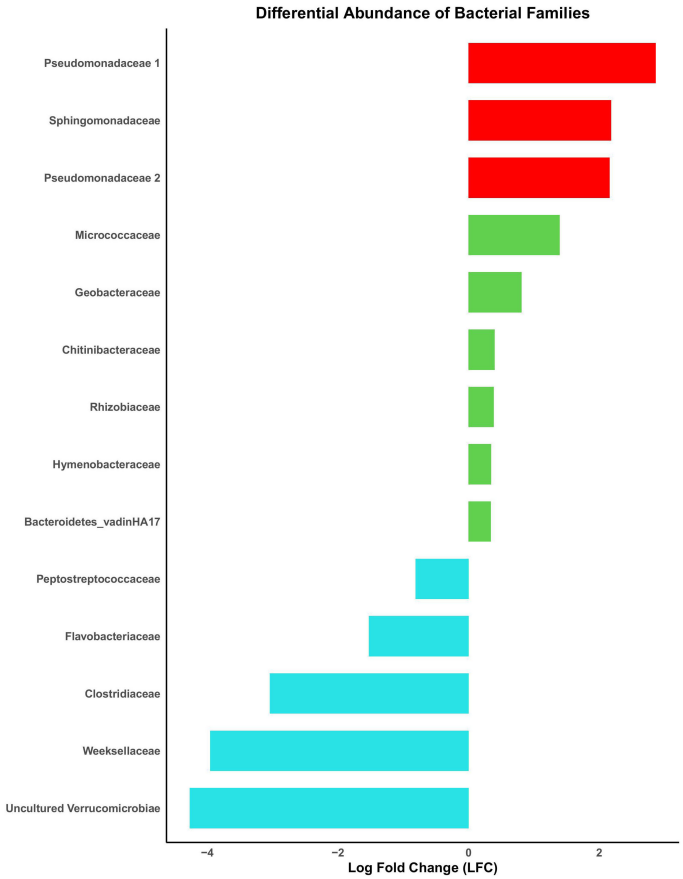

FIGURE 6
Results for the analysis of compositions of microbiomes with bias correction for *T. granulosa* which are either enriched or depreciated in the presence of high tetrodotoxin concentration. The reference for which the LFC is calculated is in respect to the high/low classification cutoff of 1 mg total newt tetrodotoxin concentration. Red ASVs are of interest for their potential tetrodotoxin production. Green ASVs are enriched in 'High-tetrodotoxin' environments, and blue are depreciated in 'High-tetrodotoxin' environments. No microbes were enriched or depreciated for *T. torosa*.

et al., 2023). Our findings also suggest that TTX may help shape the newt skin microbiome, but not fungal pathogen dynamics. However, these patterns were inconsistent across the two *Taricha* newt species in our study. For *T. granulosa*, TTX was correlated with skin microbiome composition, but not in *T. torosa*. These variable results between the newt species may be explained by differences in the microecosystem that symbionts experience on the skin of the two species, given that TTX concentration is generally higher in *T. granulosa* compared to *T. torosa* (this study; Johnson et al., 2018). Another inconsistent result between the two *Taricha* newt species was the relationship between Bd infection and the skin microbiomes. While Bd infection presence explained variation in skin microbiome structure in *T. torosa*, this pattern was not observed in *T. granulosa*. One explanation for this result could be that the *T. torosa* microbiome is able to adapt and respond to chytrid infection as a defensive function (Woodhams et al., 2023). *Taricha granulosa* skin microbiomes were not associated with Bd infection in our study, despite similar infection in both species; lack of microbiome adaptability in response to chytrid infection in *T. granulosa* could potentially contribute to Bd susceptibility differences between *T. granulosa* and *T. torosa*. Manipulative experiments specifically testing this hypothesis in each newt species would be needed to evaluate microbiome response to chytrid infection in relation to disease susceptibility and severity.

In contrast to Johnson et al. (2018), we did not detect a correlation between TTX concentration and Bd infection in this study. Johnson et al. (2018) identified a negative relationship between TTX concentration and Bd infection, such that higher TTX concentrations correlated with lower Bd infection prevalence in both *T. granulosa* and *T. torosa*. Our findings, combined with Johnson et al. (2018), could point to a more complicated relationship at a macroecological scale for both *T. granulosa* and *T. torosa*. For example, our sampling effort for Bd was conducted once at each of our respective sites, with only 58% of sites positive for Bd infection; thus, these results are only a snapshot into this system. The patterns between Bd and TTX likely vary with spatiotemporal context, including Bd infection seasonality and TTX concentration ephemerality with newt breeding season (Kriger and Hero, 2007; Bucciarelli et al., 2016). TTX bioavailability within the amphibian microecosystem is not in stasis, with TTX concentrations within a population displaying spatiotemporal variation in annually recaptured *T. torosa* in respect to sex, breeding site fidelity, and sampling time (Bucciarelli et al., 2016, 2017; Frey et al., 2023). Furthermore, toxin concentrations

10.3389/famrs.2024.1503056

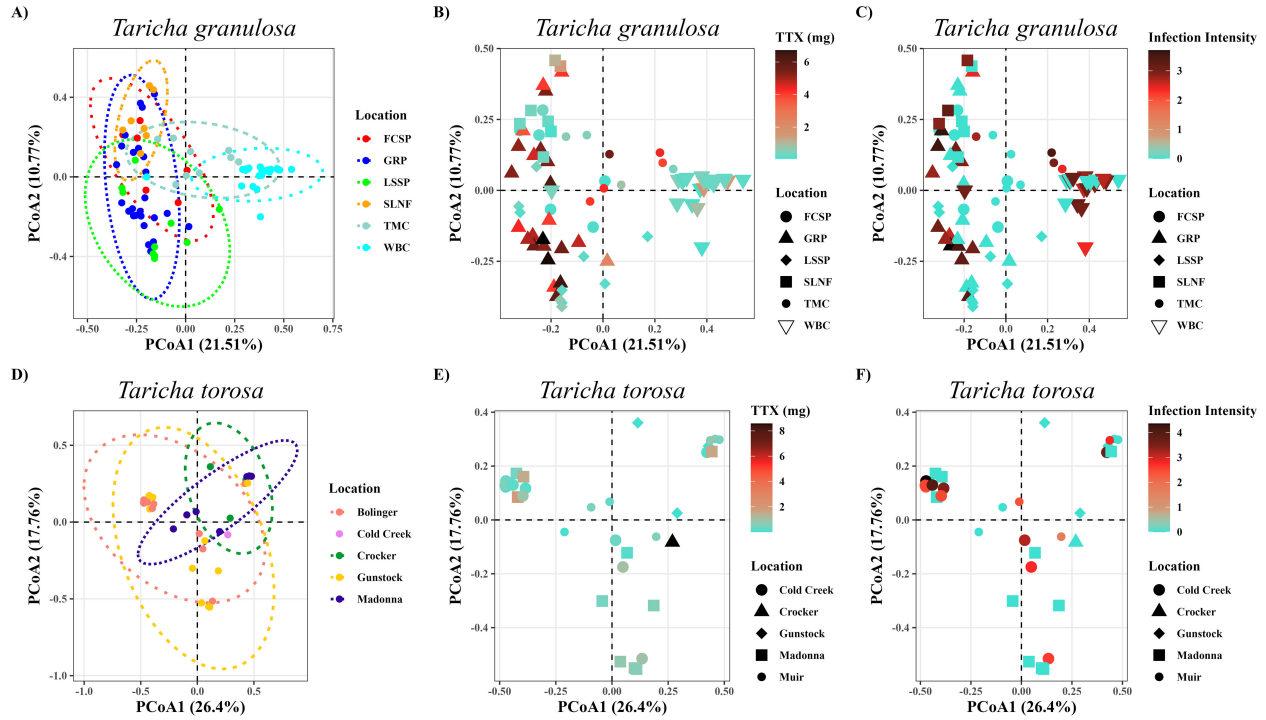

FIGURE 7
PCoA ordination plots using QIIME2 derived Bray-Curtis distance matrices for *T. granulosa* (top) and *T. torosa* (bottom). **(A, D)** Location ordination with colors representing each respective location, **(B, E)** tetrodotoxin concentration (mg) as a gradient with shapes delineating location, **(C, F)** Bd infection intensity (ITS copy number) as a presence/absence with shapes delineating location. This pattern repeats on the bottom.

TABLE 3 PERMANOVA using QIIME2 derived microbiome beta diversity metrics by categorical variables: Bd infection presence/absence, tetrodotoxin high/low classification, location, and sex; PERMANOVA test statistic provided is Pseudo-F. Mantel test using beta matrices against numerical variables: Bd infection intensity, tetrodotoxin (mg), and mass; Mantel test statistic provided is Spearman rho.

	Taricha granulosa								*Taricha torosa*							
	Bray-Curtis		Jaccard		Weighted-Unifrac		Unweighted-Unifrac		Bray-Curtis		Jaccard		Weighted-Unifrac		Unweighted-Unifrac	
Category	Test statistic	p-value	Test statistic	p-value	Test statistic	p-value	Test statistic	p-value	Test statistic	p-value	Test statistic	p-value	Test statistic	p-value	Test statistic	p-value
TTX (high/low)	3.78	**0.001**	5.06	**0.001**	4.96	**0.004**	8.41	**0.001**	0.77	0.66	0.94	0.6	0.46	0.77	0.73	0.8
TTX (mg)	-0.05	0.28	-0.01	0.75	0.06	0.09	0.01	0.9	0.17	0.06	0.08	0.66	-0.02	0.22	0.01	0.9
Bd (Presence/Absence)	1.11	0.29	1.37	0.1	1.92	0.11	1.64	0.07	4.67	**0.001**	2.19	**0.001**	1.95	0.11	2.45	**0.005**
Bd Infection Intensity (All Samples)	-0.03	0.61	-0.02	0.7	0.008	0.85	-0.1	0.08	0.22	**0.002**	0.2	**0.004**	0.12	0.09	0.12	0.062
Bd Infection Intensity (Bd Positive Only)	-0.13	0.11	-0.12	0.13	-0.04	0.57	-0.13	0.41	0.12	0.45	0.12	0.43	0.15	0.19	0.11	0.37
Location	6.91	**0.001**	6.41	**0.001**	6.36	**0.001**	6.91	**0.001**	6.46	**0.001**	2.55	**0.001**	5.83	**0.001**	3.19	**0.001**

(Continued)

TABLE 3 Continued

	Taricha granulosa								*Taricha torosa*							
	Bray-Curtis		Jaccard		Weighted-Unifrac		Unweighted-Unifrac		Bray-Curtis		Jaccard		Weighted-Unifrac		Unweighted-Unifrac	
Sex	0.62	0.91	0.87	0.64	0.48	0.76	0.73	0.73	1.24	0.23	0.93	0.65	0.59	0.63	1.18	0.24
Mass	0.09	0.1	0.07	0.15	0.08	**0.02**	0.04	0.31	0.19	**0.02**	0.114	**0.02**	0.31	**0.002**	0.06	0.44

Bold values indicate significance p > 0.05.

TABLE 4 Relative frequency tables of *T. granulosa* and *T. torosa* were paired against the Vaelli et al. (2020) data set of known tetrodotoxin-producing bacteria. The ASV richness column represents unique matches to the tetrodotoxin-producing microbe dataset at a particular location. The reads column indicates the cumulative abundance of observed ASVs at that location. The relative abundance column represents the cumulative number of matched reads at that particular location divided by the cumulative number of reads for that location multiplied by 100 to obtain a percentage. The tetrodotoxin (mg) column represents the mean tetrodotoxin concentration at that location.

Taricha granulosa						*Taricha torosa*					
Location		ASV Richness	Reads	Relative Abundance (%)	Mean TTX (mg)	Location		ASV Richness	Reads	Relative Abundance (%)	Mean TTX (mg)
FCSP	(n=7)	3	42	0.27	0.16	Bolinger	(n=1)	2	2	0.05	0.16
GRP	(n=25)	4	309	0.56	4.9	Cold Creek	(n=11)	4	116	0.31	0.42
LSSP	(n=10)	4	249	1.13	0.3	Crocker	(n=1)	3	60	1.58	8.58
SLNF	(n=7)	1	7	0.019	0.57	Gunstock	(n=6)	4	843	4.44	0.009
TMC	(n=10)	4	59	0.27	2.69	Madonna	(n=12)	3	172	0.45	0.8
WBC	(n=24)	4	10397	19.69	0.42	Muir	(n=9)	5	586	1.87	0.64

TABLE 5 Linear regression model using Vsearch matches with a 99% threshold as a predictor variable against tetrodotoxin concentration as a response variable.

Taricha granulosa				*Taricha torosa*			
ASV	Coef	t-value	p-value	ASV	Coef	t-value	p-value
TX174011	-0.06	-2.47	**0.02**	TX174011	-26.39	0.44	0.66
TX111008	-0.166	-1.08	0.72	TX111008	-26.754	-0.97	0.35
TX135003	-0.029	-1.18	0.24	TX135003	33.666	1.55	0.13
TX174011	0.039	0.36	0.72	TX196002	30.394	1.24	0.23
-	-	-	-	**TX180013**	**-32.609**	**-0.93**	**0.36**
-	-	-	-	**TX111009**	**15.693**	**0.75**	**0.46**

ASV corresponds to the name of the isolate within the Vaelli et al. (2020) dataset. Two ASVs (in bold) which were classified in this study matched to the same ASV from the Vaelli et al. (2020) dataset.

can be variable in response to sampling stress, and subsequently increase or remain low depending on sampling regimes (Bucciarelli et al., 2016). Repeat sampling examining seasonal TTX concentration and TTX bioavailability in association with seasonal changes within the microbiome are necessary to fully understand this relationship. Further studies with repeated sampling and larger sample sizes paired alongside laboratory work to examine *in vivo* interactions among host-possessed TTX, microbiome structure, and Bd infection could prove critical in further parsing intricacies within this system.

Many studies have attempted to identify the origin of TTX associated with eukaryotic hosts, including production by host-associated microbes (e.g., Chau et al., 2011; Magarlamov et al., 2017; Kudo et al., 2020, 2021). Our results only partially support this TTX production hypothesis. We did not find positive correlations between TTX concentration and relative abundance of TTX-producing skin bacteria described by Vaelli et al. (2020); however, TTX-producing microbes may be present and not yet identified within our samples, and expansion of known TTX-producing microbes to this dataset would be useful for predictive

capabilities. In fact, we observed a negative correlation between overall abundance of putative TTX-producers and actual TTX concentration on individuals. However, relative abundance of several taxa that were previously described as TTX producers (Pseudomonadaceae, Sphingomonadaceae) (Vaelli et al., 2020) were significantly greater on newts with higher TTX concentrations. In addition, TTX-producing bacteria were identified on all body sites on the *Taricha* newts, but not detected in soil samples. While our results do not support a direct relationship between TTX concentration and richness of known TTX-producing ASVs, this could further support the existence of environmental or conditional requirements for TTX production within microbial communities (Magarlamov et al., 2017). Given the low abundance of TTX produced by bacterial cultures compared to that detected on newt skin (Vaelli et al., 2020), an alternate hypothesis is that TTX is sequestered over time or perhaps during certain seasons and is thus not always correlated with TTX-producing bacteria on the skin at a given sampling time point. Many microbial members of the newt microbiomes have not been tested for TTX production, and those taxa that have been tested have experienced set culturing conditions rather than realistic environmental conditions; it is therefore likely that there are other bacterial symbionts contributing to TTX production that are yet unknown. The abundance of one TTX-producing taxa could also outweigh the influence of another TTX-producing taxa and may indicate unobserved interactions within the microecosystem which influence our results. Our analyses were often performed using a single predictor variable, but with greater data availability and finer scale resolution regarding these dynamics, multivariate analysis may further refine our understanding of this system.

Interestingly, we found a greater diversity of matches to the known TTX-producing microbe dataset for *T. torosa* (*Pseudomonas, Aeromonas, Shewanella*) than in *T. granulosa* (*Pseudomonas*), even with the dataset created using microbes from *T. granulosa* (Vaelli et al., 2020). Potential TTX production by such families as Pseudomonadaceae and Sphingomonadaceae within the newt skin microecosystem presents an opportunity to investigate the genetic elements and the necessary conditions for TTX production by these lineages. For example, TTX production by bacteria could involve specific gene(s) or biosynthetic gene clusters (Chau et al., 2011, 2013; Kudo et al., 2014), located on either chromosomes or plasmids. In addition, toxin production genes could be located on prophage, which is the case for the diphtheria toxin-encoding prophage in *Vibrio cholerae* (Feiner et al., 2015). Comparative whole genome sequencing of potential TTX producers compared to related non-TTX producers may reveal the genetic elements required for TTX production. Further, resource availability or limitations within the microecosystem can play a role in gene expression (Balakrishnan et al., 2021), which may prompt microbes to produce and release TTX within the system (Chau et al., 2011). Further experimental work in transcriptomics is needed to understand the context under which TTX might be produced by bacteria.

Location was consistently correlated among species with the dynamics we observed for TTX concentration, Bd infection prevalence, and microbiome structure for both newt species; however, location alone does not entirely explain the dynamics we observe among all our documented variables. Geographic isolation among populations is considered a primary factor concerning TTX and its evolutionary influence on competing newt and snake species. The predation of garter snakes on newts has historically been considered the primary driver of toxin concentration, and this predation varies among locations, but predation alone does not explain the unknown mechanism by which TTX is manufactured within this system nor the emergence of TTX within the system 100 million years before intense competition began between newts and garter snakes (Gendreau et al., 2021). This is further confounded by the discovery of ephemerality of toxin concentration with season, life stage, and stress (Bucciarelli et al., 2016; Frey et al., 2023), similar to changes observed in microbiome structure (Kueneman et al., 2014; Walke et al., 2021). Given documented variation of toxin concentration by location, it is important to note that an individual newt at a particular site could foster a great abundance of toxin-producing microbes within its microbiome and not possess expected levels of toxin concentration, potentially indicating a limiting factor or stressor necessary to induce commensurate toxin levels. Genetic limitations of individual newts may play a role in this variation as several mutations to voltage-gated sodium channels are necessary to harbor the toxin and have been found to be commensurate with toxin concentrations (Vaelli et al., 2020; Gendreau et al., 2021).

We found that endogenous host-associated toxins can shape the newt skin microbiome and may influence infection by pathogens. Our study indicates a necessity to further investigate tetrodotoxin and its associations within the newt microecosystem with a more longitudinal focus as a single sampling time point approach is insufficient to explain the dynamics we observe concerning toxin concentration, microbiome structure, and pathogen infection. Spatiotemporal variation among each component which make up the newt-TTX holobiont entity indicates a complex set of interactions currently unexplained by traditional concepts. Our study illustrates complexity concerning host-pathogen, toxin-microbiome, and toxin-pathogen interactions; furthermore, studies which examine systems including host-associated toxins as a component of the microecosystem should not disregard its potential to influence study results.

Data availability statement

The data presented in the study are deposited in the NCBI SRA repository, accession number PRJNA1188619. Data analysis code is available at https://github.com/Talon-Jost/TTX-Bd-Microbiome.git.

Ethics statement

The animal study was approved by the Washington State University IACUC and the University of California, Los Angeles IACUC. The study was conducted in accordance with the local legislation and institutional requirements.

Author contributions

TJ: Conceptualization, Data curation, Formal analysis, Funding acquisition, Methodology, Visualization, Writing – original draft, Writing – review & editing. AHe: Conceptualization, Investigation, Writing – original draft. BL: Data curation, Formal analysis, Investigation, Methodology, Validation, Writing – review & editing. KM: Formal analysis, Visualization, Writing – review & editing. AS: Data curation, Investigation, Resources, Supervision, Validation, Writing – review & editing. DB: Data curation, Investigation, Writing – review & editing. AHo: Conceptualization, Writing – review & editing. MB: Conceptualization, Formal analysis, Writing – review & editing. OH-G: Conceptualization, Validation, Writing – review & editing. GB: Investigation, Resources, Validation, Writing – review & editing. DW: Conceptualization, Resources, Supervision, Writing – review & editing. JP-S: Conceptualization, Formal analysis, Resources, Supervision, Validation, Writing – review & editing. JW: Conceptualization, Methodology, Resources, Supervision, Writing – review & editing.

Funding

The author(s) declare financial support was received for the research, authorship, and/or publication of this article. U.S. Department of Education Graduate Assistance in Areas of National Need (GAANN) grant to Eastern Washington University and TJ (Award Number: P200A210129). President's Associates Student Research Scholarship to DB (CSU Bakersfield: P031M190029). Graduate Student-Faculty Collaborative Research Program to DB and AS (CSUB Title Vb). Washington State University School of Biological Sciences Elling Award and William and Mary Graber Sciences Scholarship to AHe. U.S. National Science Foundation (IOS-1845634) to DW.

Acknowledgments

The authors would like to thank Megan Bryant, Sky Button, Jared Lamm, Hailee Leimbach-Maus, and Macee Mitchell for their help conducting lab work, field work and support in operations. The authors would also like to thank Jessica Allen, Heather Eisthen, and Patrick Vaelli for their technical support. We would like to thank our funding sources: Title Vb GCRP, the President's Associates at CSUB, The Department of Education, Washington State University, and the National Science Foundation.

Conflict of interest

The authors declare that the research was conducted in the absence of any commercial or financial relationships that could be construed as a potential conflict of interest.

Generative AI statement

The author(s) declare that no Generative AI was used in the creation of this manuscript.

Publisher's note

Supplementary material

The Supplementary Material for this article can be found online at: https://www.frontiersin.org/articles/10.3389/famrs.2024.1503056/full#supplementary-material

SUPPLEMENTARY FIGURE 1
Analysis of Vaelli et al. (2020) data of predicted tetrodotoxin-producing bacterial reads across host body habitats and environmental soil at two locations, Idaho and Oregon. Violin plots are modified to include points representing each sample.

SUPPLEMENTARY FIGURE 2
Effects of tetrodotoxin exposure doses (in μM) on the growth of *Batrachochytrium dendrobatidis* (Bd) and *B. salamandrivorans* (Bsal). Error bars represent the standard error of the average percent growth for Bd and Bsal, respectively.

References

Balakrishnan, R., de Silva, R. T., Hwa, T., and Cremer, J. (2021). Suboptimal resource allocation in changing environments constrains response and growth in bacteria. *Molec. Syst. Biol.* 17, e10597. doi: 10.15252/msb.202110597

Beck, M. W. (2017). *ggord: Ordination Plots with ggplot2. R package version*, Vol. 1. 595.

Bell, S. C., Alford, R. A., Garland, S., Padilla, G., and Thomas, A. D. (2013). Screening bacterial metabolites for inhibitory effects against *Batrachochytrium dendrobatidis* using a spectrophotometric assay. *Dis. Aquat. Org* 103, 77–85. doi: 10.3354/dao02560

Berger, L., Speare, R., Daszak, P., Green, D. E., Cunningham, A. A., Goggin, C. L., et al. (1998). Chytridiomycosis causes amphibian mortality associated with population declines in the rain forests of Australia and Central America. *Proc. Natl. Acad. Sci.* 95, 9031–9036. doi: 10.1073/pnas.95.15.9031

Bisanz, J. E. (2018). *qiime2R: Importing QIIME2 artifacts and associated data into R sessions. Version 0.99.K.* Available online at: https://github.com/jbisanz/qiime2R.

Bokulich, N. A., Subramanian, S., Faith, J. J., Gevers, D., Gordon, J. I., Knight, R., et al. (2013). Quality-filtering vastly improves diversity estimates from Illumina amplicon sequencing. *Nat. Methods* 10, 57–59. doi: 10.1038/nmeth.2276

Bolger, A. M., Lohse, M., and Usadel, B. (2014). Trimmomatic: A flexible trimmer for Illumina sequence data. *Bioinformatics* 30, 2114–2120. doi: 10.1093/bioinformatics/btu170

Bolyen, E., Rideout, J. R., Dillon, M. R., Bokulich, N. A., Abnet, C. C., Al-Ghalith, G. A., et al. (2019). Reproducible, interactive, scalable and extensible microbiome data science using QIIME 2. *Nat. Biotechnol.* 37, 852–857. doi: 10.1038/s41587-019-0209-9

Boyle, D., Boyle, D., Olsen, V., Morgan, J., and Hyatt, A. (2004). Rapid quantitative detection of chytridiomycosis (*Batrachochytrium dendrobatidis*) in amphibian samples using real-time Taqman PCR assay. *Dis. Aquat. Organ.* 60, 141–148. doi: 10.3354/dao060141

Brodie, E. D., and Brodie, E. D. (1990). Tetrodotoxin resistance in garter snakes: An evolutionary response of predators to dangerous prey. *Evolution* 44, 651–659. doi: 10.1111/j.1558-5646.1990.tb05945.x

Brodie, E. D., Feldman, C. R., Hanifin, C. T., Motychak, J. E., Mulcahy, D. J., Williams, B. L., et al. (2005). Parallel arms races between garter snakes and newts involving tetrodotoxin as the phenotypic interface of coevolution. *J. Chem. Ecol.* 31, 343–356. doi: 10.1007/s10886-005-1345-x

Brodie, E. D., Ridenhour, B. J., and Brodie, E. D. (2002). The evolutionary response of predators to dangerous prey: Hotspots and coldspots in the geographic mosaic of coevolution between garter snakes and newts. *Evolution* 56, 2067–2082. doi: 10.1111/j.0014-3820.2002.tb00132.x

Bucciarelli, G. M., Green, D. B., Shaffer, H. B., and Kats, L. B. (2016). Individual fluctuations in toxin levels affect breeding site fidelity in a chemically defended amphibian. *Proc. R. Soc B Biol. Sci.* 283, 20160468. doi: 10.1098/rspb.2016.0468

Bucciarelli, G. M., Li, A., Kats, L. B., and Green, D. B. (2014). Quantifying tetrodotoxin levels in the California newt using a non-destructive sampling method. *Toxicon* 80, 87–93. doi: 10.1016/j.toxicon.2014.01.009

Bucciarelli, G. M., Shaffer, H. B., Green, D. B., and Kats, L. B. (2017). An amphibian chemical defense phenotype is inducible across life history stages. *Sci. Rep.* 7, 8185. doi: 10.1038/s41598-017-08154-z

Bucciarelli, G. M., Smith, S. J., Choe, J. J., Shin, P. D., Fisher, R. N., and Kats, L. N. (2023). Native amphibian toxin reduces invasive crayfish feeding with potential benefits to stream biodiversity. *BMC Ecol. Evo.* 23, 51. doi: 10.1186/s12862-023-02162-6

Buttimer, S., Hernández-Gómez, O., and Rosenblum, E. B. (2022). Skin bacterial metacommunities of San Francisco Bay Area salamanders are structured by host genus and habitat quality. *FEMS Microbiol. Ecol.* 97, fiab162. doi: 10.1093/femsec/fiab162

Calhoun, D. M., Bucciarelli, G. M., Kats, L. B., Zimmer, R. K., and Johnson, P. T. J. (2017). Noxious newts and their natural enemies: Experimental effects of tetrodotoxin exposure on trematode parasites and aquatic macroinvertebrates. *Toxicon* 137, 120–127. doi: 10.1016/j.toxicon.2017.07.021

Caporaso, J. G., Lauber, C. L., Walters, W. A., Berg-Lyons, D., Huntley, J., Fierer, N., et al. (2012). Ultra-high-throughput microbial community analysis on the Illumina HiSeq and MiSeq platforms. *ISME J.* 6, 1621–1624. doi: 10.1038/ismej.2012.8

Caporaso, J. G., Lauber, C. L., Walters, W. A., Berg-Lyons, D., Lozupone, C. A., Turnbaugh, P. J., et al. (2011). Global patterns of 16S rRNA diversity at a depth of millions of sequences per sample. *Proc. Natl. Acad. Sci.* 108, 4516–4522. doi: 10.1073/pnas.1000080107

Cardall, B. L., Brodie, E. D., Brodie, E. D., and Hanifin, C. T. (2004). Secretion and regeneration of tetrodotoxin in the rough-skin newt (*Taricha granulosa*). *Toxicon* 44, 933–938. doi: 10.1016/j.toxicon.2004.09.006

Chau, R., Kalaitzis, J. A., and Neilan, B. A. (2011). On the origins and biosynthesis of tetrodotoxin. *Aquat. Toxicol.* 104, 61–72. doi: 10.1016/j.aquatox.2011.04.001

Chau, R., Kalaitzis, J. A., Wood, S. A., and Neilan, B. A. (2013). Diversity and biosynthetic potential of culturable microbes associated with toxic marine animals. *Mar. Drugs* 11, 2695–2712. doi: 10.3390/md11082695

Custer, G. F., Gans, M., van Diepen, L. T. A., Dini-Andreote, F., and Buerkle, C. A. (2023). Comparative analysis of core microbiome assignments: Implications for ecological synthesis. *mSystems* 8, e01066–e01022. doi: 10.1128/msystems.01066-22

Davis, N. M., Proctor, D. M., Holmes, S. P., Relman, D. A., and Callahan, B. J. (2018). Simple statistical identification and removal of contaminant sequences in marker-gene and metagenomics data. *Microbiome* 6, 1–14. doi: 10.1186/s40168-018-0605-2

Downes, H. (1995). Tricaine anesthesia in Amphibia: A review. *Bull. Assoc. Reptil. Amphib. Vet.* 5, 11–16. doi: 10.5818/1076-3139.5.2.11

Ewels, P., Magnusson, M., Lundin, S., and Käller, M. (2016). MultiQC: summarize analysis results for multiple tools and samples in a single report. *Bioinformatics* 32, 3047–3048. doi: 10.1093/bioinformatics/btw354

Feiner, R., Argov, T., Rabinovich, L., Sigal, N., Borovok, I., and Herskovits, A. A. (2015). A new perspective on lysogeny: prophages as active regulatory switches of bacteria. *Nat. Rev. Microbiol.* 13, 641–650. doi: 10.1038/nrmicro3527

Frey, A. R., Bucciarelli, G. M., Hu, D. D., Kats, L. B., and Green, D. B. (2023). An amphibian toxin phenotype is sexually dimorphic and shows seasonal concordant change between sexes. *Front. Amphib. Reptile Sci.* 1. doi: 10.3389/famrs.2023.1279848

Gall, B. G., Stokes, A. N., Brodie, E. D., and Brodie, E. D. (2022). Tetrodotoxin levels in lab-reared rough-skinned newts (*Taricha granulosa*) after 3 years and comparison to wild-caught juveniles. *Toxicon* 213, 7–12. doi: 10.1016/j.toxicon.2022.04.007

Gall, B. G., Stokes, A. N., French, S. S., Brodie, E. D., and Brodie, E. D. (2012). Female newts (*Taricha granulosa*) produce tetrodotoxin laden eggs after long term captivity. *Toxicon* 60, 1057–1062. doi: 10.1016/j.toxicon.2012.07.017

Gendreau, K. L., Hornsby, A. D., Hague, M. T. J., and McGlothlin, J. W. (2021). Gene conversion facilitates the adaptive evolution of self-resistance in highly toxic newts. *Mol. Biol. Evol.* 38, 4077–4094. doi: 10.1093/molbev/msab182

Hanifin, C. T. (2010). The chemical and evolutionary ecology of tetrodotoxin (TTX) toxicity in terrestrial vertebrates. *Mar. Drugs* 8, 577–593. doi: 10.3390/md8030577

Hanifin, C. T., Brodie, E. D., and Brodie, E. D. (2004). A predictive model to estimate total skin tetrodotoxin in the newt *Taricha granulosa*. *Toxicon* 43, 243–249. doi: 10.1016/j.toxicon.2003.11.025

Hanifin, C. T., Brodie, E. D. Jr., and Brodie, E. D. III (2008). Phenotypic mismatches reveal escape from arms-race coevolution. *PloS Biol.* 6, e60. doi: 10.1371/journal.pbio.0060060

Harris, R. N., Brucker, R. M., Walke, J. B., Becker, M. H., Schwantes, C. R., Flaherty, D. C., et al. (2009). Skin microbes on frogs prevent morbidity and mortality caused by a lethal skin fungus. *ISME J.* 3, 818–824. doi: 10.1038/ismej.2009.27

Hernández-Gómez, O., Wuerthner, V., and Hua, J. (2020). Amphibian host and skin microbiota response to a common agricultural antimicrobial and internal parasite. *Microb. Ecol.* 79, 175–191. doi: 10.1007/s00248-019-01351-5

Jani, A. J., and Briggs, C. J. (2014). The pathogen *Batrachochytrium dendrobatidis* disturbs the frog skin microbiome during a natural epidemic and experimental infection. *Proc. Natl. Acad. Sci.* 111, E5049–E5058. doi: 10.1073/pnas.1412752111

Jiménez, R. R., Carfagno, A., Linhoff, L., Gratwicke, B., Woodhams, D. C., Chafran, L. S., et al. (2022). Inhibitory bacterial diversity and mucosome function differentiate susceptibility of Appalachian salamanders to chytrid fungal infection. *Appl. Environ. Microbiol.* 88, e01818–e01821. doi: 10.1128/aem.01818-21

Johnson, P. T. J., Calhoun, D. M., Stokes, A. N., Susbilla, C. B., McDevitt-Galles, T., Briggs, C. J., et al. (2018). Of poisons and parasites—the defensive role of tetrodotoxin against infections in newts. *J. Anim. Ecol.* 87, 1192–1204. doi: 10.1111/1365-2656.12816

Katoh, K., Misawa, K., Kuma, K. I., and Miyata, T. (2002). MAFFT: a novel method for rapid multiple sequence alignment based on fast Fourier transform. *Nucleic Acids Res.* 30, 3059–3066. doi: 10.1093/nar/gkf436

Kohl, K. D., and Dearing, M. D. (2016). The woodrat gut microbiota as an experimental system for understanding microbial metabolism of dietary toxins. *Front. Microbiol.* 7. doi: 10.3389/fmicb.2016.01165

Kriger, K. M., and Hero, J.–. M. J. -.-M. (2007). Large-scale seasonal variation in the prevalence and severity of chytridiomycosis. *J. Zool.* 271, 352–359. doi: 10.1111/j.1469-7998.2006.00220.x

Kudo, Y., Hanifin, C. T., Kotaki, Y., and Yotsu-Yamashita, M. (2020). Structures of N-hydroxy-type tetrodotoxin analogues and bicyclic guanidinium compounds found in toxic newts. *J. Nat. Prod.* 83, 2706–2717. doi: 10.1021/acs.jnatprod.0c00623

Kudo, Y., Hanifin, C. T., and Yotsu-Yamashita, M. (2021). Identification of tricyclic guanidino compounds from the tetrodotoxin-bearing newt *Taricha granulosa*. *Org. Lett.* 23, 3513–3517. doi: 10.1021/acs.orglett.1c00916

Kudo, Y., Yamashita, Y., Mebs, D., Cho, Y., Konoki, K., Yasumoto, T., et al. (2014). C5–C10 directly bonded tetrodotoxin analogues: possible biosynthetic precursors of tetrodotoxin from newts. *Angew. Chem. Int. Ed.* 53, 14546–14549. doi: 10.1002/anie.201408913

Kueneman, J. G., Parfrey, L. W., Woodhams, D. C., Archer, H. M., Knight, R., and McKenzie, V. J. (2014). The amphibian skin-associated microbiome across species, space and life history stages. *Mol. Ecol.* 23, 1238–1250. doi: 10.1111/mec.12510

Lago, J., Rodríguez, L., Blanco, L., Vieites, J., and Cabado, A. (2015). Tetrodotoxin, an extremely potent marine neurotoxin: distribution, toxicity, origin and therapeutical uses. *Mar. Drugs* 13, 6384–6406. doi: 10.3390/md13106384

Lauer, A., Simon, M. A., Banning, J. L., André, E., Duncan, K., and Harris, R. N. (2007). Common cutaneous bacteria from the eastern red-backed salamander can inhibit pathogenic fungi. *Copeia* 3, 630–640. doi: 10.1371/journal.pone.0010957

Lehman, E. M., Brodie, E. D., and Brodie, E. D. (2004). No evidence for an endosymbiotic bacterial origin of tetrodotoxin in the newt *Taricha granulosa*. *Toxicon* 44, 243–249. doi: 10.1016/j.toxicon.2004.05.019

Li, Z., Wang, Q., Sun, K., and Feng, J. (2021). Prevalence of *Batrachochytrium dendrobatidis* in amphibians from 2000 to 2021: A global systematic review and meta-analysis. *Front. Vet. Sci.* 8. doi: 10.3389/fvets.2021.791237

Lin, H., and Peddada, S. D. (2020). Analysis of compositions of microbiomes with bias correction. *Nat. Commun.* 11, 3514. doi: 10.1038/s41467-020-17041-7

Longford, S. R., Campbell, A. H., Nielsen, S., Case, R. J., Kjelleberg, S., and Steinberg, P. D. (2019). Interactions within the microbiome alter microbial interactions with host chemical defences and affect disease in a marine holobiont. *Sci. Rep.* 9, 1363. doi: 10.1038/s41598-018-37062-z

Magarlamov, T., Melnikova, D., and Chernyshev, A. (2017). Tetrodotoxin-producing bacteria: Detection, distribution and migration of the toxin in aquatic systems. *Toxins* 9, 166. doi: 10.3390/toxins9050166

Martel, A., Spitzen-van der Sluijs, A., Blooi, M., Bert, W., Ducatelle, R., Fisher, M. C., et al. (2013). *Batrachochytrium salamandrivorans* sp. nov. causes lethal chytridiomycosis in amphibians. *Proc. Natl. Acad. Sci.* 110, 15325–15329. doi: 10.1073/pnas.1307356110

Miyazawa, K., and Noguchi, T. (2001). Distribution and origin of tetrodotoxin. *J. Toxicol. Toxin Rev.* 20, 11–33. doi: 10.1081/TXR-100103081

Moczydlowski, E. G. (2013). The molecular mystique of tetrodotoxin. *Toxicon* 63, 165–183. doi: 10.1016/j.toxicon.2012.11.026

Nguyen, L. T., Schmidt, H. A., Von Haeseler, A., and Minh, B. Q. (2015). IQ-TREE: A fast and effective stochastic algorithm for estimating maximum-likelihood phylogenies. *Mol. Biol. Evol.* 32, 268–274. doi: 10.1093/molbev/msu300

Parada, A. E., Needham, D. M., and Fuhrman, J. A. (2016). Every base matters: assessing small subunit rRNA primers for marine microbiomes with mock communities, time series and global field samples. *Environ. Microbiol.* 18, 1403–1414. doi: 10.1111/1462-2920.13023

Pebesma, E., and Bivand, R. (2023). *Spatial data science: With applications in R. Chapman and Hall/CRC.*

Pebesma, E. J., Mailund, T., and Hiebert, J. (2016). Measurement Units in R. *R J.* 8, 489–494. doi: 10.32614/RJ-2016-061

Pedregosa, F., Varoquaux, G., Gramfort, A., Michel, V., Thirion, B., Grisel, O., et al. (2011). Scikit-learn: machine learning in Python. *J. Mach. Learn.* 12, 2825–2830. doi: 10.5555/1953048.2078195

Piovia-Scott, J., Pope, K., Joy Worth, S., Rosenblum, E. B., Poorten, T., Refsnider, J., et al. (2015). Correlates of virulence in a frog-killing fungal pathogen: Evidence from a California amphibian decline. *ISME J.* 9, 1570–1578. doi: 10.1038/ismej.2014.241

Pratheepa, V., Alex, A., Silva, M., and Vasconcelos, V. (2016). Bacterial diversity and tetrodotoxin analysis in the viscera of the gastropods from Portuguese coast. *Toxicon* 119, 186–193. doi: 10.1016/j.toxicon.2016.06.003

Quast, C., Pruesse, E., Yilmaz, P., Gerken, J., Schweer, T., Yarza, P., et al. (2012). The SILVA ribosomal RNA gene database project: Improved data processing and web-based tools. *Nucleic Acids Res.* 41, D590–D596. doi: 10.1093/nar/gks1219

Quince, C., Lanzen, A., Davenport, R. J., and Turnbaugh, P. J. (2011). Removing noise from pyrosequenced amplicons. *BMC Bioinform.* 12, 1–18. doi: 10.1186/1471-2105-12-38

R Core Team (2023). *R: a language and environment for statistical computing* (Vienna, Austria: R Foundation for Statistical Foundation). Available at: https://www.R-project.org (accessed May 21, 2024).

Rebollar, E. A., Martínez-Ugalde, E., and Orta, A. H. (2020). The amphibian skin microbiome and its protective role against chytridiomycosis. *Herpetologica* 76, 167–177. doi: 10.1655/0018-0831-76.2.167

Reimche, J. S., Brodie, E. D., Stokes, A. N., Ely, E. J., Moniz, H. A., Thill, V. L., et al. (2020). The geographic mosaic in parallel: Matching patterns of newt tetrodotoxin levels and snake resistance in multiple predator–prey pairs. *J. Anim. Ecol.* 89, 1645–1657. doi: 10.1111/1365-2656.13212

Rognes, T., Flouri, T., Nichols, B., Quince, C., and Mahé, F. (2016). VSEARCH: a versatile open source tool for metagenomics. *PeerJ* 4, e2584. doi: 10.7717/peerj.2584

Roth, T., Foley, J., Worth, J., Piovia-Scott, J., Pope, K., and Lawler, S. (2013). Bacterial flora on Cascades frogs in the Klamath Mountains of California. *Comp. Immunol. Microbiol. Infect. Dis.* 36, 591–598. doi: 10.1016/j.cimid.2013.07.002

Scheele, B. C., Pasmans, F., Skerratt, L. F., Berger, L., Martel, A., Beukema, W., et al. (2019). Amphibian fungal panzootic causes catastrophic and ongoing loss of biodiversity. *Science* 363, 1459–1463. doi: 10.1126/science.aav0379

Sewell, T. R., Longcore, J., and Fisher, M. C. (2021). *Batrachochytrium dendrobatidis. Trends Parasitol.* 37, 933–934. doi: 10.1016/j.pt.2021.04.014

Stokes, A. N., Ray, A. M., Buktenica, M. W., Gall, B. G., Paulson, E., Paulson, D., et al. (2015). Otter predation on *Taricha granulosa* and variation in tetrodotoxin levels with elevation. *Northwest. Nat.* 96, 13–21. doi: 10.1898/NWN13-19.1

Stokes, A. N., Williams, B. L., and French, S. S. (2012). An improved competitive inhibition enzymatic immunoassay method for tetrodotoxin quantification. *Biol. Proceed. Online* 14, 1–5. doi: 10.1186/1480-9222-14-3

Theis, K. R., Dheilly, N. M., Klassen, J. L., Brucker, R. M., Baines, J. F., Bosch, T. C. G., et al. (2016). Getting the hologenome concept right: an eco-evolutionary framework for hosts and their microbiomes. *mSystems* 1, e00028–e00016. doi: 10.1128/mSystems.00028-16

Thumsová, B., González-Miras, E., Faulkner, S. C., and Bosch, J. (2021). Rapid spread of a virulent amphibian pathogen in nature. *Biol. Invasions* 23, 3151–3160. doi: 10.1007/s10530-021-02571-y

Tsuda, K., and Kawamura, M. (1952). The constituents of the ovaries of globefish. VI Purification of globefish poison by chromatography. *Yakugaku Zasshi* 72, 771–773. doi: 10.1248/yakushi1947.72.6_771

Vaelli, P. M., Theis, K. R., Williams, J. E., O'Connell, L. A., Foster, J. A., and Eisthen, H. L. (2020). The skin microbiome facilitates adaptive tetrodotoxin production in poisonous newts. *eLife* 9, e53898. doi: 10.5061/dryad.pg4f4qrk1

Walke, J. B., Becker, M. H., Hughey, M. C., Swartwout, M. C., Jensen, R. V., and Belden, L. K. (2015). Most of the dominant members of amphibian skin bacterial communities can be readily cultured. *Appl. Environ. Microbiol.* 81, 6589–6600. doi: 10.1128/AEM.01486-15

Walke, J. B., Becker, M. H., Krinos, A., Chang, E. A. B., Santiago, C., Umile, T. P., et al. (2021). Seasonal changes and the unexpected impact of environmental disturbance on skin bacteria of individual amphibians in a natural habitat. *FEMS Microbiol. Ecol.* 97, fiaa248. doi: 10.1093/femsec/fiaa248

Walke, J. B., Becker, M. H., Loftus, S. C., House, L. L., Cormier, G., Jensen, R. V., et al. (2014). Amphibian skin may select for rare environmental microbes. *ISME J.* 8, 2207–2217. doi: 10.1038/ismej.2014.77

Walters, W., Hyde, E. R., Berg-Lyons, D., Ackermann, G., Humphrey, G., Parada, A., et al. (2015). Improved bacterial 16S rRNA gene (V4 and V4-5) and fungal internal transcribed spacer marker gene primers for microbial community surveys. *mSystems* 1, 1128. doi: 10.1128/mSystems.00009-15

Williams, B. L., Hanifin, C. T., Brodie, E. D., and Brodie, E. D. (2012). Predators usurp prey defenses? Toxicokinetics of tetrodotoxin in common garter snakes after consumption of rough-skinned newts. *Chemoecology* 22, 179–185. doi: 10.1007/s00049-011-0093-3

Williams, B. L., Powers, L. V., and Garner, M. M. (2016). A pufferfish (*Tetradon nigroviridis*) available in the common pet trade harbors lethal concentrations of tetrodotoxin: a case study of poisoning in a cuvier's dwarf caiman (*Paleosuchus palpebrosus*). *J. Zoo. Wildl. Med.* 47, 676–680. doi: 10.1638/2015-0077.1

Woodhams, D. C., Brandt, H., Baumgartner, S., Kielgast, J., Küpfer, E., Tobler, U., et al. (2014). Interacting symbionts and immunity in the amphibian skin mucosome predict disease risk and probiotic effectiveness. *PloS One* 9, e96375. doi: 10.1371/journal.pone.0096375

Woodhams, D. C., McCartney, J., Walke, J. B., and Whetstone, R. (2023). The adaptive microbiome hypothesis and immune interactions in amphibian mucus. *Dev. Comp. Immunol.* 145, 104690. doi: 10.1016/j.dci.2023.104690

Yap, T. A., Nguyen, N. T., Serr, M., Shepack, A., and Vredenburg, V. T. (2017). *Batrachochytrium salamandrivorans* and the risk of a second amphibian pandemic. *EcoHealth* 14, 851–864. doi: 10.1007/s10393-017-1278-1

Yu, J., Jiang, C., Yamano, R., Koike, S., Sakai, Y., Mino, S., et al. (2023). Unveiling the early life core microbiome of the sea cucumber *Apostichopus japonicus* and the unexpected abundance of the growth-promoting Sulfitobacter. *Anim. Microbiome* 5, 54. doi: 10.1186/s42523-023-00276-2

Zepeda Mendoza, M. L., Xiong, Z., Escalera-Zamudio, M., Runge, A. K., Thézé, J., Streicker, D., et al. (2018). Hologenomic adaptations underlying the evolution of sanguivory in the common vampire bat. *Nat. Ecol. Evol.* 2, 659–668. doi: 10.1038/s41559-018-0476-8

Zilber-Rosenberg, I., Rosenberg, E., Koren, O., Reshef, L., and Efrony, R. (2007). The role of microorganisms in coral health, disease and evolution. *Nat. Rev. Microbiol.* 5, 355–362. doi: 10.1038/nrmicro1635